Supporting Information for:

Recipient Plasma Metabolomics as a Predictor of Heart Transplant Severe Primary Graft Dysfunction

Joshua D. Preston, BS[1,2], Clayton J. Rust, MD[1], Aubrey C. Reed, BS[1], Supreet S. Randhawa, MS[1], Ailin Tang, BS[1], Kimberly A. Rooney, BS[3], Misho Kozmava, BS[3], Jaclyn Weinberg, BS[2], Lucy Avant, BS[1], Catherine L.B. McGeoch, MD, MSc[1], Gustavo A. Parrilla, MD[1], Jiada Zhan, BS, RD[2], ViLinh Tran, MS[2], Michael E. Halkos, MD, MSc[1], Muath M. Bishawi, MD PhD[1], Mani A. Daneshmand, MD[1], Arshed A. Quyyumi, MD[3], Charles D. Searles, MD[3], Young-Mi Go, PhD[2], Dean P. Jones, PhD[2], Joshua L. Chan, MD[1]

[1]Division of Cardiothoracic Surgery, Department of Surgery, Emory University School of Medicine, Atlanta, GA, USA

[2]Division of Pulmonary, Allergy, Critical Care, and Sleep Medicine, Department of Medicine, Emory University School of Medicine, Atlanta, GA, USA

[3]Division of Cardiology, Department of Medicine, Emory University School of Medicine, Atlanta, GA, USA

Table of Contents

Supplementary Figure S1 2

Supplementary Figure S2.1 3

Supplementary Figure S2.2 4

Supplementary Figure S2.3 5

Supplementary Figure S2.4 6

Supplementary Figure S2.5 7

Expanded Metabolomics Methods and Other Technical Details 8-9

Sample Collection and Processing 8

Metabolomics Profiling with Liquid Chromatography-Mass Spectrometry 8

Feature Extraction, Annotation, and Identification 8-9

Quality Control and Data Transformation 9

Statistical Analysis and Data Visualization 9-10

Partial Least Squares Discriminant Analysis and Volcano Plots 9

Pathway Enrichment Analysis 9-10

Identified and Annotated Metabolite Analysis 10

Sensitivity Analysis 10

References 11-12

Supplementary Figure S1

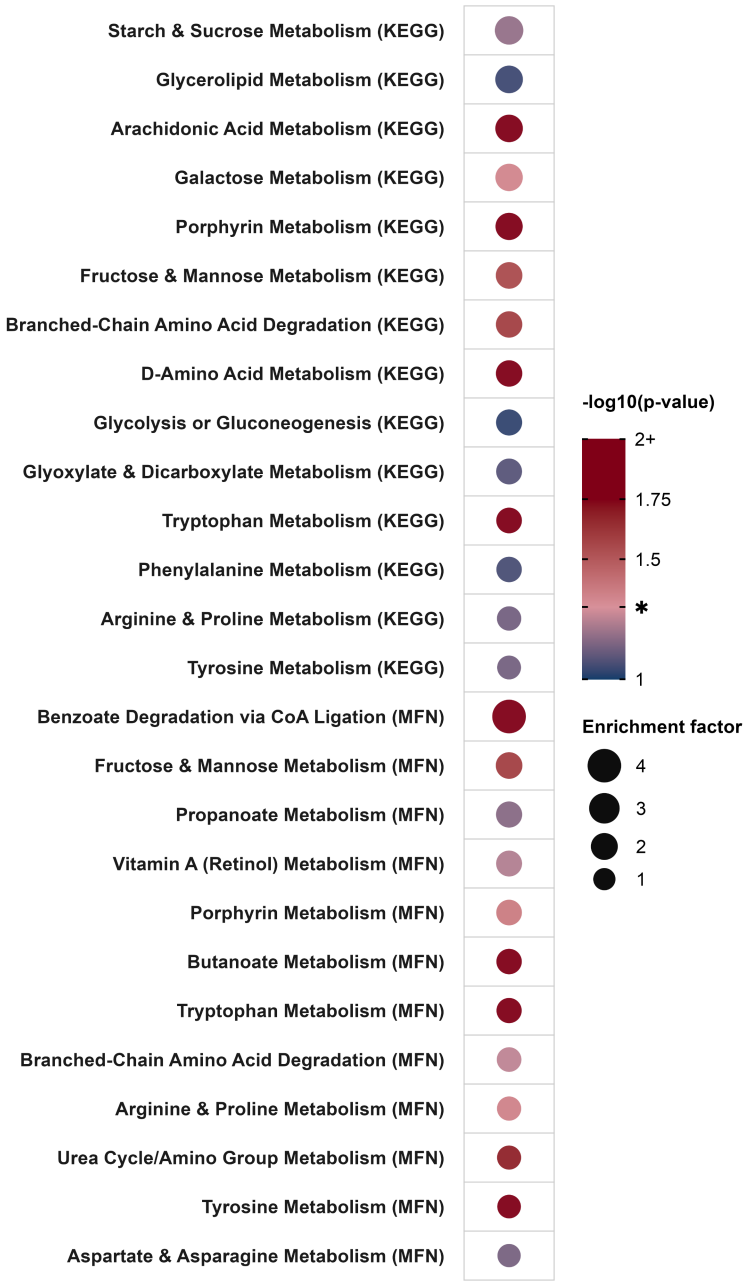

** Corresponding point to p = 0.05*

Supplementary Figure S2.1

Markers on x-axis indicate Y/N severe PGD status.

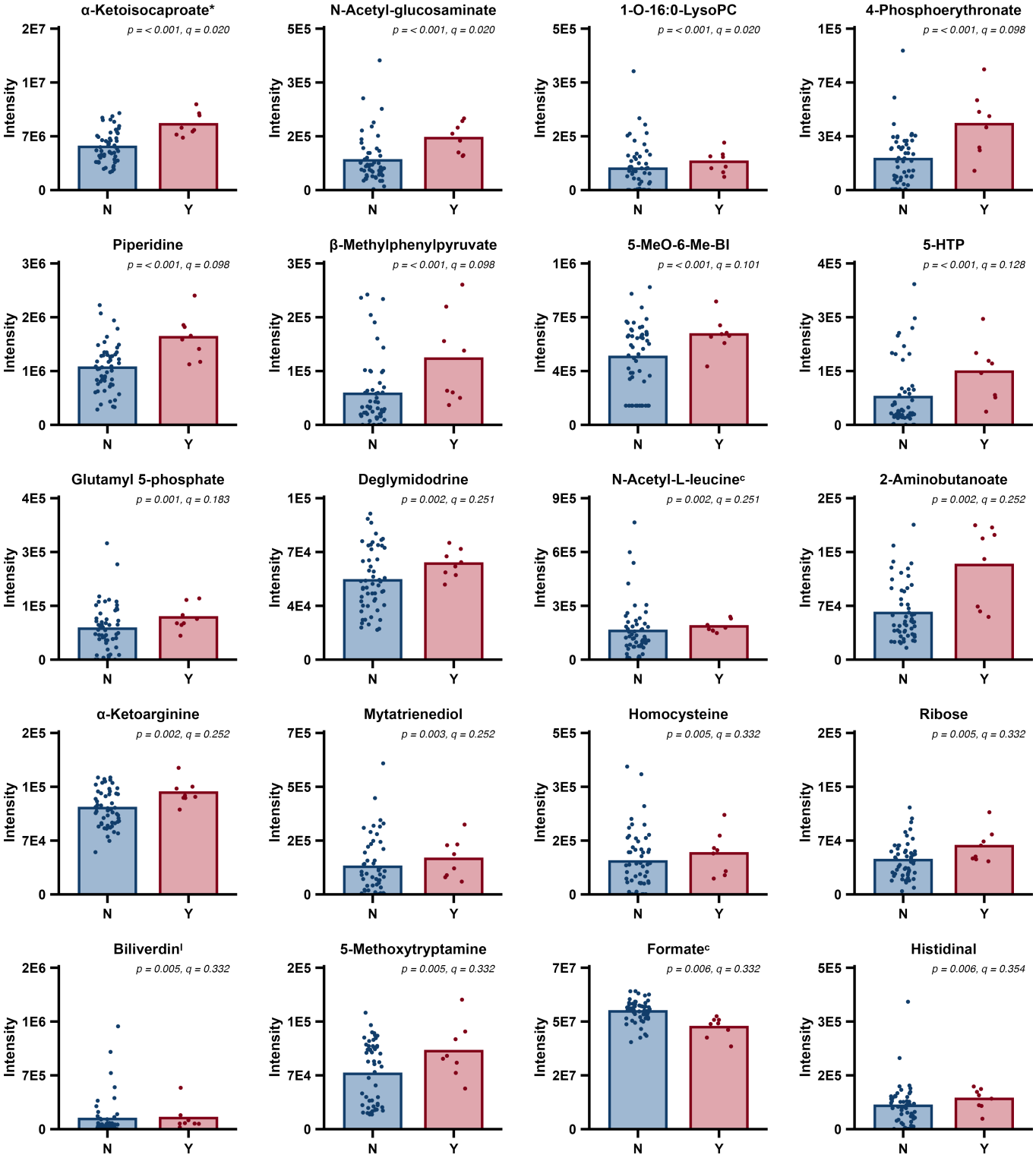

** M-H adduct presented but also identified with authentic standard as M-H+HCOONa adduct; see Figure.Row.Column S2.2.2.3.*

[c] Identity confirmed with authentic chemical standard.

[l] Isomer annotated or isomer present in library of authentic chemical standards; see Supplementary Figure S2.5 for details.

Supplementary Figure S2.2

Markers on x-axis indicate Y/N severe PGD status.

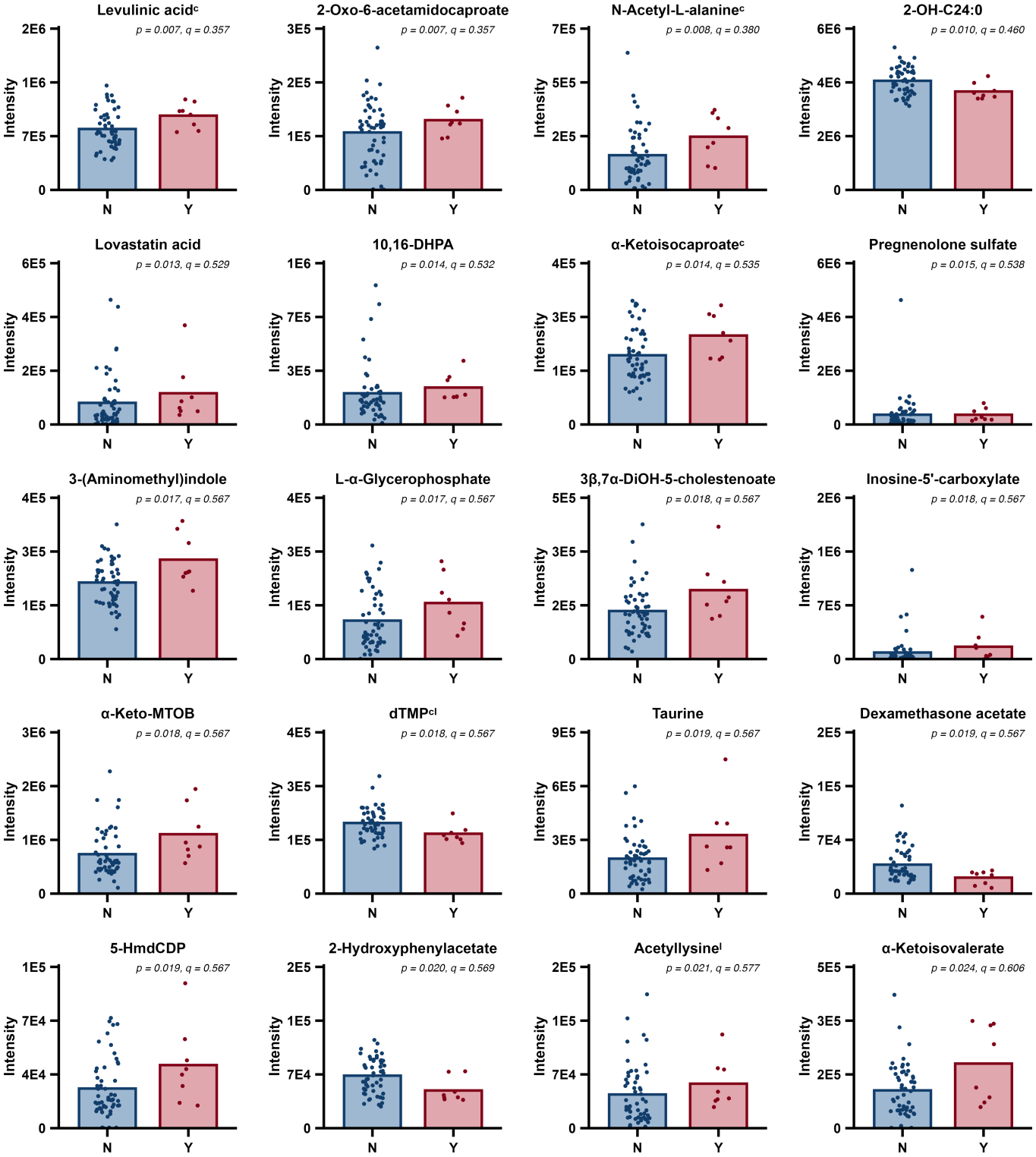

[c] *Identity confirmed with authentic chemical standard.*

[l] *Isomer annotated or isomer present in library of authentic chemical standards; see Supplementary Figure S2.5 for details.*

Supplementary Figure S2.3

Markers on x-axis indicate Y/N severe PGD status.

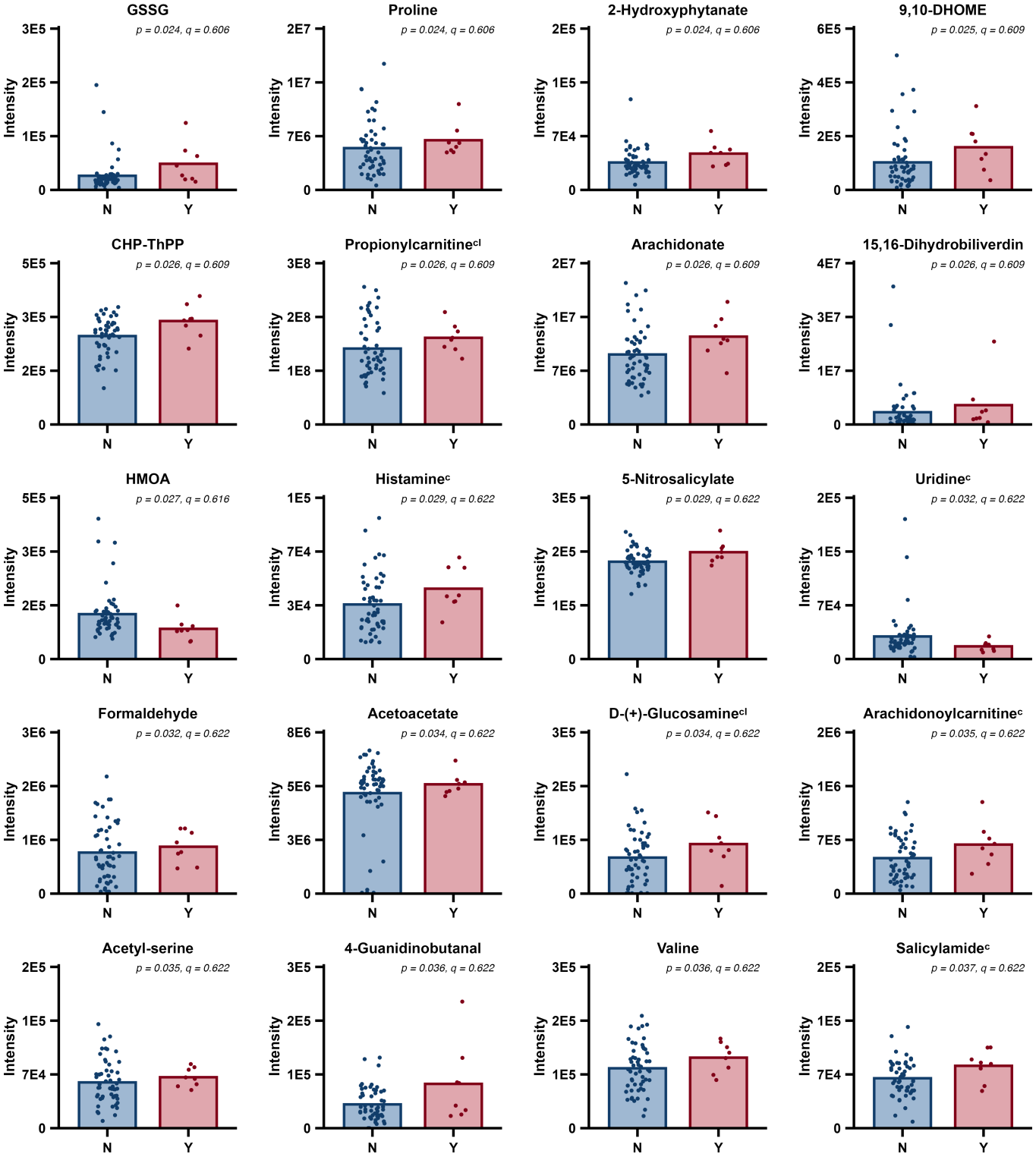

[c] *Identity confirmed with authentic chemical standard.*

[l] *Isomer annotated or isomer present in library of authentic chemical standards; see Supplementary Figure S2.5 for details.*

Supplementary Figure S2.4

Markers on x-axis indicate Y/N severe PGD status.

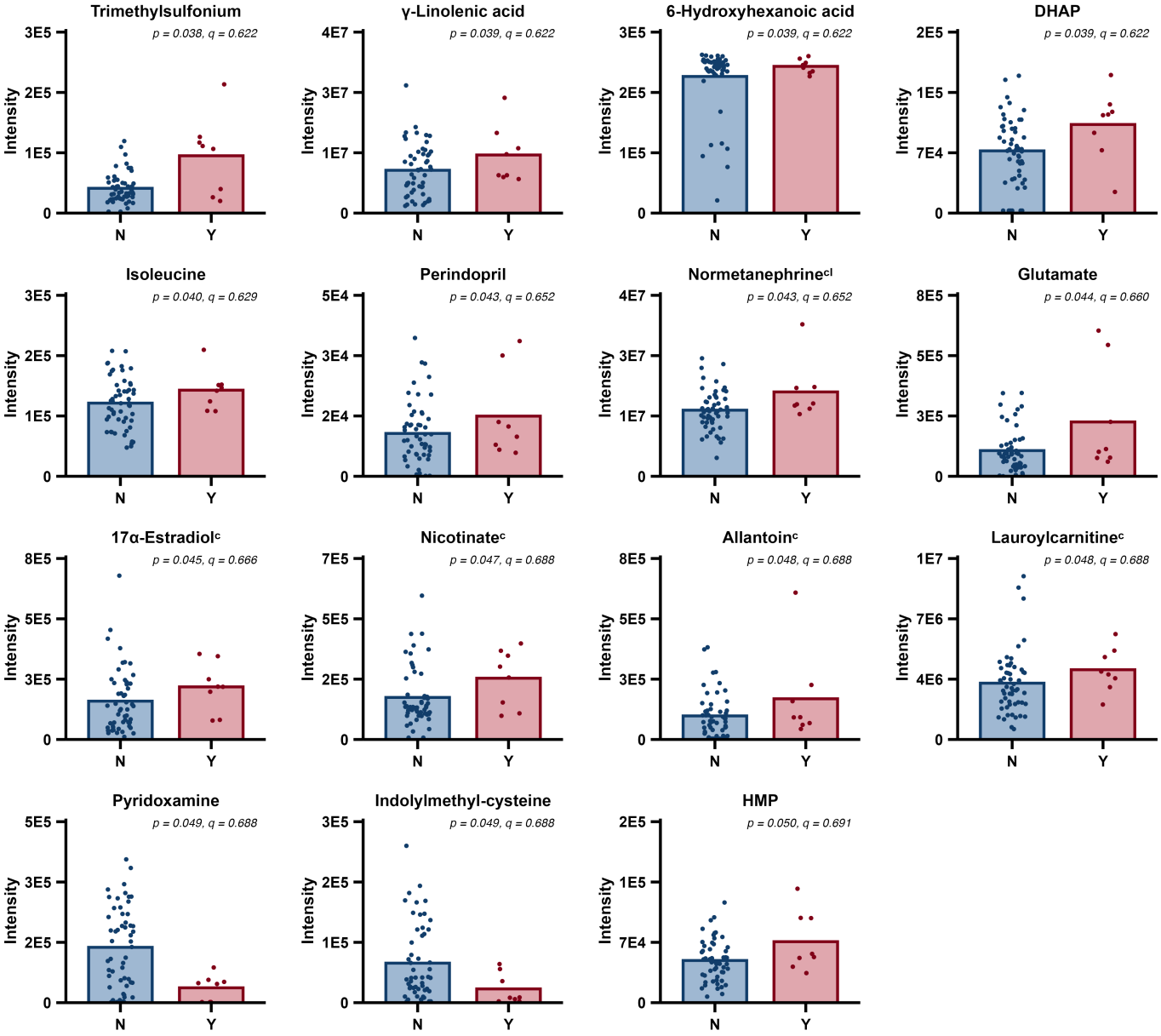

[c] *Identity confirmed with authentic chemical standard.*

[l] *Isomer annotated or isomer present in library of authentic chemical standards; see Supplementary Figure S2.5 for details.*

Supplementary Figure S2.5

Abbreviations and Adducts Table

Figure.Row.Column	Abbreviated/Displayed Name	Longform, Other, or Isomer Name(s)	Adduct
S2.1.1.1	α-Ketoisocaproate*	-	M-H
S2.1.1.2	N-Acetyl-glucosaminate	-	M-H+HCOONa
S2.1.1.3	1-O-16:0-LysoPC	1-O-Hexadecyl-lyso-sn-glycero-3-phosphocholine	M+FA-H
S2.1.1.4	4-Phosphoerythronate	-	M-H
S2.1.2.1	Piperidine	-	M+H
S2.1.2.2	β-Methylphenylpyruvate	(3S)-2-Oxo-3-phenylbutanoate	M-H+HCOONa
S2.1.2.3	5-MeO-6-Me-BI	5-Methoxy-6-methylbenzimidazole	M+H
S2.1.2.4	5-HTP	5-Hydroxy-L-tryptophan	M-H
S2.1.3.1	Glutamyl 5-phosphate	-	M-H
S2.1.3.2	Deglymidodrine	-	M+H
S2.1.3.3	N-Acetyl-L-leucine[c]	-	M+H
S2.1.3.4	2-Aminobutanoate	-	M+H-NH3
S2.1.4.1	α-Ketoarginine	5-Guanidino-2-oxopentanoate	M-H
S2.1.4.2	Mytatrienediol	-	M+H
S2.1.4.3	Homocysteine	-	M+2Na-H
S2.1.4.4	Ribose	-	M+H-2H2O
S2.1.5.1	Biliverdin[I]	-	M-H
S2.1.5.2	5-Methoxytryptamine	-	M+H
S2.1.5.3	Formate[c]	-	M-H+HCOONa
S2.1.5.4	Histidinal	-	M+H
S2.2.1.1	Levulinic acid[c]	-	M-H
S2.2.1.2	2-Oxo-6-acetamidocaproate	6-Acetamido-2-oxohexanoate	M+H
S2.2.1.3	N-Acetyl-L-alanine[c]	-	M+H-H2O
S2.2.1.4	2-OH-C24:0	2-Hydroxytetracosanoic acid	M+Cl
S2.2.2.1	Lovastatin acid	-	M+Hac-H
S2.2.2.2	10,16-DHPA	10,16-Dihydroxyhexadecanoic acid	M+H
S2.2.2.3	α-Ketoisocaproate[c]	-	M-H+HCOONa
S2.2.2.4	Pregnenolone sulfate	3β-Hydroxypregn-5-en-20-one sulfate	M-H
S2.2.3.1	3-(Aminomethyl)indole	-	M+H-NH3
S2.2.3.2	L-α-Glycerophosphate	sn-Glycerol 1-phosphate	M+H
S2.2.3.3	3β,7α-DiOH-5-cholestenoate	3β,7α-Dihydroxy-5-cholestenoate	M-H
S2.2.3.4	Inosine-5'-carboxylate	-	M+H-H2O
S2.2.4.1	α-Keto-MTOB	4-Methylthio-2-oxobutanoic acid	M+Cl
S2.2.4.2	dTMP[cI]	Thymidine 5'-monophosphate	M+FA-H
S2.2.4.3	Taurine	-	M+H
S2.2.4.4	Dexamethasone acetate	Dexamethasone acetate anhydrous	M-H
S2.2.5.1	5-HmdCDP	2'-Deoxy-5-hydroxymethylcytidine-5'-diphosphate	M-H+HCOONa
S2.2.5.2	2-Hydroxyphenylacetate	-	M+H
S2.2.5.3	Acetyllysine[I]	-	M-H
S2.2.5.4	α-Ketoisovalerate	-	M+2Na-H
S2.3.1.1	GSSG	Glutathione disulfide	M+FA-H
S2.3.1.2	Proline	-	M+H
S2.3.1.3	2-Hydroxyphytanate	-	M-H
S2.3.1.4	9,10-DHOME	-	M+Hac-H
S2.3.2.1	CHP-ThPP	3-Carboxy-1-hydroxypropylthiamine diphosphate	M+Cl
S2.3.2.2	Propionylcarnitine[cI]	-	M+H+NH4
S2.3.2.3	Arachidonate	-	M-H
S2.3.2.4	15,16-Dihydrobiliverdin	-	M+H
S2.3.3.1	HMOA	4-Hydroxy-4-methyl-2-oxoadipate	M+Cl
S2.3.3.2	Histamine[c]	-	M+H
S2.3.3.3	5-Nitrosalicylate	-	M-H
S2.3.3.4	Uridine[c]	-	M-H+HCOONa
S2.3.4.1	Formaldehyde	-	M+Hac-H
S2.3.4.2	Acetoacetate	-	M-H
S2.3.4.3	D-(+)-Glucosamine[cI]	-	M+H
S2.3.4.4	Arachidonoylcarnitine[c]	-	M+H
S2.3.5.1	Acetyl-serine	-	M-H
S2.3.5.2	4-Guanidinobutanal	-	M+H
S2.3.5.3	Valine	-	M-H+HCOONa
S2.3.5.4	Salicylamide[c]	-	M-H2O-H
S2.4.1.1	Trimethylsulfonium	-	M+Hac-H
S2.4.1.2	γ-Linolenic acid	(6Z,9Z,12Z)-Octadecatrienoic acid	M-H
S2.4.1.3	6-Hydroxyhexanoic acid	-	M-H
S2.4.1.4	DHAP	Glycerone phosphate	M+H
S2.4.2.1	Isoleucine	-	M-H+HCOONa
S2.4.2.2	Perindopril	-	M-H
S2.4.2.3	Normetanephrine[cI]	-	M+H-H2O
S2.4.2.4	Glutamate	-	M-H
S2.4.3.1	17α-Estradiol[c]	-	2M-3H
S2.4.3.2	Nicotinate[c]	-	M+H
S2.4.3.3	Allantoin[c]	-	M+2Na-H
S2.4.3.4	Lauroylcarnitine[c]	-	M+H
S2.4.4.1	Pyridoxamine	-	M+Hac-H
S2.4.4.2	Indolylmethyl-cysteine	S-(Indolylmethylthiohydroximoyl)-L-cysteine	M+H
S2.4.4.3	HMP	4-Amino-5-hydroxymethyl-2-methylpyrimidine	M+H

Footnote Table

Figure.Row.Column	Abbreviated/Displayed Name	Footnote
S2.1.5.1	Biliverdin[I]	[I]Annotated isomers = Biliverdin-IX-δ and Biliverdin-IX-β (M-H adducts)
S2.2.4.2	dTMP[cI]	[I]Standard library isomers = 2'-Deoxyuridine 5'-monophosphate (M+Hac-H adduct)
S2.2.5.3	Acetyllysine[I]	[I]Annotated isomer = 6-Acetamido-3-aminohexanoate (M-H adduct)
S2.3.2.2	Propionylcarnitine[cI]	[I]Standard library isomers = 5-Aminopentanoic acid (M+H adduct)
S2.3.4.3	D-(+)-Glucosamine[cI]	[I]Standard library isomers = D-Mannosamine (M+H adduct)
S2.4.2.3	Normetanephrine[cI]	[I]Standard library isomers = 1,3-Dihydro-(2H)-indol-2-one[c] (M+CH4O+H adduct)

** M-H adduct presented but also identified with authentic standard as M-H+HCOONa adduct; see Figure.Row.Column S2.2.2.3.*

[c] Identity confirmed with authentic chemical standard.

[I] Isomer annotated or isomer present in library of authentic chemical standards. See Footnote Table for details.

Expanded Metabolomics Methods and Other Technical Details

In keeping with consensus reporting standards for metabolomics experiments,[1] we provide in-depth details as follows:

Sample Collection and Processing

Blood samples were collected immediately before transplant into K2EDTA plasma preparation tubes. Once samples were collected from patients, they were immediately placed on ice. The samples remained on ice and were centrifuged at 2500 x g for 15 minutes at 4°C within 5 hours of collection (the mean time from collection to processing for all samples = 1 hour). Following centrifugation, three aliquots were made from the supernatant, which were stored at -80°C shortly after.

Metabolomics Profiling with Liquid Chromatography-Mass Spectrometry

High-resolution metabolomics was performed in the Emory Clinical Biomarkers Laboratory as previously described.[2] Plasma samples were thawed, and 10 µL of plasma was added to 190 µL of acetonitrile containing 2% internal standards. Samples were then vortexed and allowed to incubate on ice for 30 minutes. Following incubation, samples were centrifuged at 20,817 x g for 10 minutes at 4°C. Supernatants were then transferred into autosampler vials. These were loaded onto autosampler plates and were kept at -20°C until analysis. Pooled control plasma (Equitech-Bio, SHP45) and National Institute of Standards and Technology (NIST) reference plasma were prepared and analyzed in tandem.

Metabolomics analysis was conducted with a liquid chromatography-mass spectrometry system (LC-MS) consisting of a Vanquish Duo UHPLC coupled to an Orbitrap ID-X Tribrid Mass Spectrometer (Thermo Scientific). Autosampler plates containing samples were maintained at 4°C in the autosampler of the LC-MS throughout the analysis. Samples were analyzed in triplicate on a 5-min method using C18 chromatography coupled to negative electrospray ionization (ESI) (C18-) and hydrophilic interaction liquid chromatography coupled to positive ESI (HILIC+). Analyte separation for HILIC was performed with a Waters Acquity BEH Amide HILIC column (2.1 mm x 100 mm, 1.7 µm particle size) and gradient elution with LCMS-grade solvents and additives. The HILIC mobile phases included (Buffer A) water with 1 mM ammonium acetate and 0.1% formic acid and (Buffer B) 95% acetonitrile with 1 mM ammonium acetate and 0.1% formic acid. For the HILIC gradient, an initial 0.5 min hold at 90% B was followed by a linear decrease to 20% B from 0.6 to 2.55 min, a 2 min hold, and a 5-min re-equilibration period. C18 chromatography was performed on a Thermo Hypersil Gold C18 column (2.1 mm x 100 mm, 1.9 µm particle size). The C18 mobile phases included (Buffer A) water with 1 mM ammonium acetate and (Buffer B) 99% acetonitrile with 1 mM ammonium acetate. For the C18 gradient, an initial 0.5 min hold at 1% B was followed by a 0.75 min linear increase to 99% B, held for 3.75 min, and a 5-min re-equilibration period. The flow rate for both methods was 0.3 mL/min, and the column compartment was heated to 45 °C. The mass spectrometer was operated at 120k resolution and MS1 scans were collected for *m/z* 85-1,275. Tune parameters consisted of sheath gas at 50, auxiliary gas at 10, and sweep gas at 1. The spray voltage was set to 3.50 kV for ESI+ and -2.75 kV for ESI-.

Feature Extraction, Annotation, and Identification

ProteoWizard v3[3] was used to convert raw spectral files to .mzXML files. Untargeted feature tables were then generated from extracted data using established laboratory workflows, software[4–6] (namely, apLCMS and xMSAnalyzer), and an in-house R package, *MetaboJanitoR*, which is available upon request. All feature tables were corrected for batch effects using ComBat[7] from the *sva* package.[8]

Untargeted feature tables were comprised of all HILIC+ and C18- features observed with a unique mass-to-charge ratio (*m/z*) and corresponding retention time (RT). Identified/annotated feature tables were

made up of Level 1[9] and Level 3[9] identifications. Level 1 identifications were obtained by ion dissociation mass spectrometry relative to authentic standards (mass error = ± 5 ppm, retention time threshold = ± 30 seconds). Level 3 identifications were made using an in-house annotation algorithm (see https://github.com/jamesjiadazhan for the future release of this R package upon its publication), which generates annotations based on precursor-product correlations (note: this version of the algorithm chose a single best adduct for the feature table based on the strength of the precursor-product correlation alone). All raw data files (.mzXML format) and untargeted feature tables analyzed for this study will be available on October 31, 2026, through the NIH Common Fund's National Metabolomics Data Repository (NMDR) website, Metabolomics Workbench (Project ID PR002742; Study ID ST004328; Project DOI http://dx.doi.org/10.21228/M87549).

Quality Control and Data Transformation

Features that were not detected in at least 80% of samples were excluded from analysis, but were included as background for pathway enrichment analysis. All '0' values (indicating non-detection by the instrument) were replaced with ½ the minimum value for that feature detected across all samples.[10] Following this, all intensity (peak area) values were $\log_2$-transformed prior to further analysis. Features in identified/annotated feature tables that significantly differed between study groups (Severe PGD versus No Severe PGD) were manually inspected and evaluated for biological plausibility and annotation quality control. Only annotated features encompassing endogenous, microbiome-derived, or relevant pharmacological metabolites were retained for analysis and visualization.

Statistical Analysis and Data Visualization

The complete analytical pipeline and source code used for data processing and statistical analyses are publicly available at https://github.com/jdpreston30/PGD-preop-metabolomics. A containerized Docker image of the complete computational environment is available at Docker Hub (https://hub.docker.com/r/jdpreston30/pgd-preop-metabolomics), and the archived analysis pipeline is permanently available at Zenodo (https://doi.org/10.5281/zenodo.17875844).

Data were analyzed and visualized using Microsoft Excel (Mac v16.101.294, Microsoft Corporation, 2025), R (v4.5.1),[11] and MetaboAnalyst (v6.0)[12] via the *MetaboAnalystR* package.[13,14] All code was written, compiled, and run in Visual Studio Code (v1.104.2, Microsoft Corporation, 2025). All data visualizations were created using *ggplot2*,[15] *igraph*,[16–18] and *ggraph*.[19] All figures were compiled using *cowplot*.[20] Epidemiologic statistics were performed using the *TernTablesR* package.[21] For all analyses, statistical significance was set at $\alpha = 0.05$.

Partial Least Squares Discriminant Analysis and Volcano Plots

Partial Least Squares Discriminant Analysis (PLS-DA) was performed using the R package, *mixOmics*.[22] Volcano plots were created by calculating p-values (based on Welch's t-tests on $\log_2$-transformed data) to compare the means of each (untargeted) feature between groups, while fold changes were determined using untransformed data. All p-value calculations were performed using R's *stats* package. For purposes of visualization, p-values were then $-\log_{10}$-transformed, and fold changes were $\log_2$-transformed.

Pathway Enrichment Analysis

All pathway enrichment analysis was performed using Mummichog.[23] A full list of p-values comparing means of all features between groups was first generated in R using the *stats* package via Welch's t-tests. These features, including the *m/z*, retention time, and ESI mode, along with their corresponding p-values, were then

analyzed using the 'Functional Analysis' tool for LC-MS from MetaboAnalyst[12] (run via the *MetaboAnalystR* package[13]), which utilizes Mummichog[23] as its core algorithm. Notably, this tool allows for the usage of Mummichog v2.0, which takes into account retention time and ESI mode, whereas the original algorithm simply used *m/z*. The parameters for the pathway enrichment included the following: mixed mode, 5 ppm mass tolerance, primary ions enforced, p-value cutoff = default for top 10% of peaks, KEGG and MFN *homo sapiens* databases. A bubble plot was then constructed based on the p-values (Fisher's) and enrichment factors generated by the algorithm output.

Identified and Annotated Metabolite Analysis

For identified/annotated metabolites, Welch's t-tests were employed to determine the p-values comparing means between each group. FDR adjustments were performed using the Benjamini-Hochberg (BH) procedure. A representative set of various families of metabolites was selected and displayed in the main text figures (**Figure 3A-D**), but all significantly differing annotated or identified features are displayed in **Supplementary Figure S2**. Both raw p-values and FDR q-values are displayed on all plots displaying annotated/identified metabolites.

Sensitivity Analysis

Given the exploratory and hypothesis-generating nature of the untargeted metabolomics study performed herein, which measured over 20,000 individual metabolic features, a conventional power analysis is not applicable. However, we conducted a quantitative post-hoc sensitivity analysis (further details of which can be found in the GitHub repository) to determine the minimum detectable effect size based on the group sizes in our study. With 62 patients (8 with severe PGD and 54 without), we had ~80% power ($\alpha = 0.05$) to detect a minimum standardized mean difference of Cohen's $d \approx 1.08$. Based on observed within-group variance (calculated using the filtered, i.e., post-QC, untargeted feature table), the median minimum detectable fold-change was 1.87 (IQR 1.46–2.99) across all features. Considering this, this study was powered to detect very large metabolic differences between groups, which is consistent with the exploratory and hypothesis-generating design. More subtle differences would require larger cohorts in future studies.

References

1. Sumner L.W., Amberg A., Barrett D., et al. Proposed minimum reporting standards for chemical analysis: Chemical Analysis Working Group (CAWG) Metabolomics Standards Initiative (MSI). *Metabolomics*. 2007;3(3):211-221. doi:10.1007/s11306-007-0082-2

2. Liu K.H., Nellis M., Uppal K., et al. Reference standardization for quantification and harmonization of large-scale metabolomics. *Analytical Chemistry*. 2020;92(13):8836-8844. doi:10.1021/acs.analchem.0c00338

3. Chambers M.C., Maclean B., Burke R., et al. A cross-platform toolkit for mass spectrometry and proteomics. *Nature Biotechnology*. 2012;30(10):918-920. doi:10.1038/nbt.2377

4. Uppal K., Soltow Q.A., Strobel F.H., et al. xMSanalyzer: automated pipeline for improved feature detection and downstream analysis of large-scale, non-targeted metabolomics data. *BMC Bioinformatics*. 2013;14(1):15. doi:10.1186/1471-2105-14-15

5. Jarrell Z.R., Smith M.R., Hu X., et al. Plasma acylcarnitine levels increase with healthy aging. *Aging*. 2020;12(13):13555-13570. doi:10.18632/aging.103462

6. Yu T., Park Y., Johnson J.M., Jones D.P. apLCMS—adaptive processing of high-resolution LC/MS data. *Bioinformatics*. 2009;25(15):1930-1936. doi:10.1093/bioinformatics/btp291

7. Johnson W.E., Li C., Rabinovic A. Adjusting batch effects in microarray expression data using empirical Bayes methods. *Biostatistics (Oxford, England)*. 2007;8(1):118-127. doi:10.1093/biostatistics/kxj037

8. Leek J.T., Johnson W.E., Parker H.S., Jaffe A.E., Storey J.D. The sva package for removing batch effects and other unwanted variation in high-throughput experiments. *Bioinformatics (Oxford, England)*. 2012;28(6):882-883. doi:10.1093/bioinformatics/bts034

9. Schymanski E.L., Jeon J., Gulde R., et al. Identifying small molecules via high resolution mass spectrometry: Communicating confidence. *Environmental Science & Technology*. 2014;48(4):2097-2098. doi:10.1021/es5002105

10. Wei R., Wang J., Su M., et al. Missing value imputation approach for mass spectrometry-based metabolomics data. *Scientific Reports*. 2018;8(1):663. doi:10.1038/s41598-017-19120-0

11. R: A language and environment for statistical computing. R Core Team; 2025. https://www.R-project.org/. [Accessed 10 December 2025]

12. Pang Z., Lu Y., Zhou G., et al. MetaboAnalyst 6.0: towards a unified platform for metabolomics data processing, analysis and interpretation. *Nucleic Acids Research*. 2024;52(W1):W398-W406. doi:10.1093/nar/gkae253

13. MetaboAnalystR 4.2: a unified LC-MS/MS workflow for global metabolomics and exposomics. Xia Lab; 2025. https://github.com/xia-lab/MetaboAnalystR. [Accessed 10 December 2025]

14. Pang Z., Chong J., Li S., Xia J. MetaboAnalystR 3.0: Toward an optimized workflow for global metabolomics. *Metabolites*. 2020. doi:doi: 10.3390/metabo10050186

15. Wickham H. *ggplot2: Elegant graphics for data analysis*. Second edition. Springer; 2016.

16. Csárdi G., Nepusz T. The igraph software package for complex network research. *InterJournal*. 2006;Complex Systems:1695. https://igraph.org

17. Antonov M., Csárdi G., Horvát S., et al. igraph enables fast and robust network analysis across programming languages. *arXiv preprint arXiv:231110260*. 2023. doi:10.48550/arXiv.2311.10260

18. Csárdi G., Nepusz T., Traag V., et al. igraph: Network analysis and visualization in R. 2025. doi:10.5281/zenodo.7682609

19. Pedersen T.L. ggraph: An implementation of grammar of graphics for graphs and networks. 2025. https://ggraph.data-imaginist.com

20. Wilke C.O. cowplot: Streamlined plot theme and plot annotations for 'ggplot2'. 2025.

21. Preston J.D. TernTablesR: Automated statistics and table generation for clinical research in R. 2025. https://github.com/jdpreston30/TernTablesR. [Accessed 10 December 2025]

22. Rohart F., Gautier B., Singh A., Lê Cao K.A. mixOmics: An R package for 'omics feature selection and multiple data integration. Schneidman D., ed. *PLOS Computational Biology*. 2017;13(11):e1005752. doi:10.1371/journal.pcbi.1005752

23. Li S., Park Y., Duraisingham S., et al. Predicting network activity from high throughput metabolomics. *PLoS computational biology*. 2013;9(7):e1003123. doi:10.1371/journal.pcbi.1003123